Hindawi
Geofluids
Volume 2019, Article ID 9069546, 13 pages
https://doi.org/10.1155/2019/9069546

Research Article

Uniaxial Compression Creep Relaxation and Grading of Coal Samples via Tests on the Progressive Failure Characteristics

Zuqiang Xiong[1,2], **Changsheng Song**[1,2], **Chengdong Su**[1,2], **Xiaolei Wang**[3], **Cheng Wang**[1,2] and **Yu Hao**[1,2]

[1]*School of Energy Science and Engineering, Henan Polytechnic University, Jiaozuo 454003, China*
[2]*Henan Key Laboratory for Green and Efficient Mining & Comprehensive Utilization of Mineral Resources, Jiaozuo 454003, China*
[3]*Lvliang University Department of Mining Engineering, Lüliang 033000, China*

Correspondence should be addressed to Changsheng Song; songcole@hpu.edu.cn

Received 5 July 2018; Revised 12 September 2018; Accepted 18 October 2018; Published 7 February 2019

Guest Editor: Fangtian Wang

An RMT-150B electrohydraulic servo testing system was used to perform uniaxial compression and uniaxial grading relaxation (creep) tests. The deformation, strength, and failure characteristics of the progressive failure process of coal samples under three loading modes were analyzed. The analysis results show that the prepeak stress-strain curve of the coal samples and the load relationships are not clear and that the whole compression process of coal still showed compression, elastic, yielding, and failure stages. The local stress drop characteristics during our relaxation creep grading tests showed no clear peak value and showed a yield curve with the shape of a conventional single plateau. The values of the mechanical parameters of axial compression were significantly higher than those obtained in the grade relaxation (creep) tests, which showed the mechanical parameters of coal samples with aging characteristics. In the relaxation (creep) tests, when the stress ratio was less than 70%, the relaxation (creep) characteristics of the sample were not clear. When the ratio of stress relaxation (creep) was more than 70% in the relaxation (creep) tests during displacement (stress) with a constant relaxation (creep) over the duration of the test, the evolution, development, and convergence of microcracks in the coal samples were observed. Relaxation (creep) stress was higher, failure duration was shorter, and the duration of failure was longer. For fully mechanized coal faces, increasing the support resistance and timely moving the support after coal cutting may prevent rib spalling accidents by reducing coal stress and exposure time in the front of the working face. Additionally, routine uniaxial compressive failures showed a simple form, having a clear tension-shear dual rupture surface. The staged relaxation creep failure testing of coal is more complex. The entire coal samples were divided into many thin-sheet debris via gradual collapse and shedding, and the number of cracks increased significantly, showing evident lateral expansion characteristics that are similar to the rib spalling characteristics in high coal mining working faces.

1. Introduction

When a coal body develops primary joints and fissures, it loses strength and its brittle failure characteristics worsen. When coal stress (strain) exceeds a certain critical value, microcracks continue to expand, which causes progressive failure of the coal body over time when the stress (strain) level is lower than the peak strength of the coal body (strain). A fully mechanized working face primarily exhibits a clear time-delayed progressive wall caving, indicating that coal wall spalling of the working face does not occur immediately after coal cutting; rather, it will happen after a period of time (lag) after the coal is cut. The lag time of coal wall spalling is affected by many factors, including buried depth, mining height, coal body structure, and mining technology. Coal wall spalling is prone to cause roof flaking. Serious coal wall spalling not only affects the normal production of a fully mechanized working face and damages the equipment on the working face but also threatens the safety of personnel, causing unsafe working conditions for coal mine production. Coal wall spalling is always the main factor affecting the safe operation of a fully mechanized mining face and

the realization of high yield and efficiency. The characteristics of progressive failure over time of a coal body must be considered as one of its most important mechanical characteristics. Studies on the characteristics of time-delayed progressive failure for coal rock bodies primarily consist of rheological (i.e., relaxation and creep) experiments carried out in laboratories.

1.1. Research Results of Rock Relaxation Experiments. Yang et al. conducted a uniaxial compression time-delayed failure experiment on marble and found that circumferential strain upon the occurrence of marble time-delayed failure is clearly larger than axial strain [1]. Feng et al. conducted a stress-relaxation experiment on several metamorphic rocks after applying a peak load and classified the results for these rocks as source rock burst or exciting rock burst [2]. Tang and Pan conducted a relaxation experiment on rocks under peak load deformation conditions and suggested that the stress relaxation curves of rocks under such conditions exhibit characteristics of step-like declination [3]. Li conducted an experimental study on the relaxation four types of rocks under uniaxial compression conditions, and the results indicate that the relaxation curves of these rocks were either continuous or stepwise [4]. Yang et al. conducted uniaxial and triaxial variable-stress-path relaxation and creep experiments on salt rocks and concluded that the steady creep rate of salt rocks is only a function of stress and does not depend on the load history [5]. Tian et al. conducted a series of triaxial relaxation tests on argillaceous sandstone under confining pressures and found that the relaxation stress during the fast relaxation stage increases with the initial deviatoric stress of the relaxation steps and is almost independent of the confining pressure [6]. Paraskevopoulou et al. measured similar stress-time responses at different load levels, indicating the existence of three distinct stages of stress relaxation. In the first stage, 55% to 95% of the total stress relaxation takes place [7].

1.2. Research Results of Rock Creep Experiments. Xu et al. and Liu et al. conducted experimental studies on the time-delayed characteristics of deep-buried marble in Jinping [8, 9]. Yu et al. performed conventional triaxial and comparative triaxial creep experiments on saturated silty mudstone and found that the characteristics of rock creep are different from those of rock relaxation and that stress relaxation characteristics cannot be simply derived from the creep characteristics of the rock [10]. Han et al. conducted a creep experiment on thin-layered rock with different loading directions [11]. Li conducted a triaxial compression creep experiment on a silty mudstone and found that the radial creep of rock entered a stage of accelerated creeping prior to axial creep, suggesting that it is more reasonable to determine whether creep destruction occurs to silty mudstone using the characteristics of radial creep [12]. Liu et al. conducted an experiment on the static fatigue effects with long-term loading on deep-buried marble in Jinping and proposed using the expansion index to elaborate on the deformation characteristics and failure modes of the rock samples used [13]. Wang et al. developed a new constitutive model in terms of the time fractal derivative to describe the full creep regions of granite. The proposed fractal model can characterize the creep behavior of granite especially during the accelerating stage, in which the classical models cannot predict [14]. Hamza and Stace explored the relationship between instantaneous (short-term) stiffness and creep properties and determined that confinement plays an important role in closing up rock joints and stiffening up fractured rock specimens [15]. Singh et al. discussed an approach to predict the creep behavior of rock salt using a uniaxial compression testing machine. Their proposed model can predict the stress-strain response of rock salt with a fair accuracy under both loading and unloading conditions [16]. Wang et al. conducted a self-developed triaxial creep experiment system for gas-bearing coal rock samples and suggested that the creep characteristics and the creep stress of gas-bearing coal samples are affected by confining pressure and gas pressure factors [17]. Zhang et al. employed constant axial pressure to conduct a stepwise unloading confining pressure experiment with different unloading velocities on tectonic coal and analyzed the energy variation law of coal samples during the unloading process [18]. A nonlinear elastoviscoplastic rheological model containing various deformation components is proposed, the proportion of the viscoplastic strain component in the creep strain is increased with higher deviatoric stress, and it can describe both the loading and unloading creep behavior precisely [19, 20].

The aforementioned researchers conducted creep and relaxation experiments on rock. Because of certain factors, namely, primitive joint fracture development, low strength, discreteness, and difficulties in the preparation of coal samples, our understanding of the characteristic rules of the time-delayed progressive failure of coal samples under the action of uniaxial compression staged relaxation (creep) remains insufficient. The joint effect of the coal body and the support in front of the working face means that the overlying portion of the rock layer is stable for a short time. There is a certain deformation (load) effect on the working face of coal walls, and coal bodies exhibit a time-delayed progressive wall caving phenomenon. It is necessary to study the characteristics of the time-delayed progressive failure of coal samples in a laboratory environment under different strain (stress) conditions. Based on this and using the RMT-150B electrohydraulic servo rock test system, we conducted uniaxial compression and uniaxial staged relaxation (creep) experiments on coal samples from the upper (middle) stratified layer of a coalbed in the Zhaogu no. 2 mine. We analyzed the characteristics of the time-delayed progressive deformation and destruction of these coal samples under three types of loads and acquired a deeper understanding of the mechanisms of the time-delayed progressive slab destruction of coal walls on the working face. The research results provide a reference for the prevention and treatment of time-delayed coal wall spalling on the working face of the Zhaogu no. 2 mine.

2. Characteristics of Samples and Experimental Methods

2.1. Characteristics of Samples. The coal samples were taken from the upper (middle) stratified layer of the coal wall on

working face 12011 of the Zhaogu no. 2 mine. Coal blocks with a size of approximately $25 \times 25 \times 25$ cm^3 were drilled and collected from dense holes along the vertical bedding. After water cooling, the collected samples were turned into standard test pieces with a diameter of 50 mm and a length of 100 mm. This accuracy satisfies the regulation requirements [15]. To minimize dispersion in the experimental results, we selected coal samples from the same layer that were relatively complete, without clear visual defects and with a roughly equal natural density and longitudinal wave velocity for our comparative experiments. The coal samples from the upper stratified layer were numbered as MS1–MS6, and the coal samples from the middle stratified layer were numbered as MZ1–MZ6.

2.2. Experimental Equipment. The experiments were conducted on an RMT-150B electrohydraulic servo rock test system. We adopted a 100 kN force sensor to measure the axial load; its accuracy was 1.0×10^{-3} kN. We used a 5.0 mm displacement sensor to measure the axial compression deformation and two 2.5 mm displacement sensors to measure the circumferential deformation, all with an accuracy of 1.0×10^{-3} mm. The system used has a good dynamic response function. It automatically collected the load and deformation information during the experimental process, which was displayed in real time to obtain the whole-process stress-strain curve of the uniaxial compression staged creep (relaxation) of the coal samples.

2.3. Experimental Method. The uniaxial compression experiments can be divided according to the loading type applied, which were conventional uniaxial compression, uniaxial compression staged relaxation, and uniaxial compression staged creep, as shown in Figure 1.

(1) Conventional uniaxial compression. After the coal sample was positioned, the axial and circumferential displacement sensors were adjusted and preloaded to their respective positions, and the displacement control was set to continuously apply a load at a loading velocity of 0.002 mm/s until the coal sample was completely destroyed

(2) Uniaxial compression staged relaxation. Based on the results of the conventional uniaxial compression experiments, the displacement control was set so as to observe the real-time load and deformation values at a loading velocity of 0.002 mm/s. When the load reached approximately 50% of its peak value, the axial deformation was maintained constant for the relaxation experiment, and the duration of the relaxation on each level was approximately 10 min. Then, the axial load was increased by 3 to 5 kN to conduct the relaxation experiment for the next level and repeated this process until the coal sample was destroyed

(3) Uniaxial compression staged creep. Based on the results of the conventional uniaxial compression experiments, the load control was set so as to observe the real-time load values at a loading velocity of 0.1 kN/s. When the axial load reached approximately 50% of its peak value, we maintained the axial load constant for approximately 10 min. Then, we increased the axial load by 3 to 5 kN to conduct the constant load test for the next level for approximately 10 min and repeated this procedure until the coal sample was destroyed

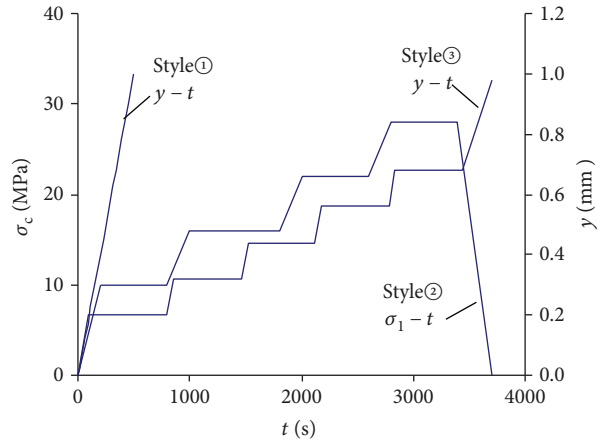

Figure 1: Schematic diagram of the three loading modes.

3. Experimental Results and Analysis

3.1. Experimental Results. Tables 1 and 2 show the results of the conventional uniaxial and staged relaxation (creep) experiments for the coal samples, respectively. In Table 1, D, H, ρ, V, σ_c, E_T, E_{50}, and μ are the diameter, height, natural density, longitudinal wave velocity, uniaxial peak strength (relaxation, creep), modulus of elasticity, deformation modulus, and Poisson's ratio of the coal sample, respectively.

Table 1 shows that the mechanical parameters of the coal samples obtained for the three loading types have some discreteness. To intuitively reflect this feature, Figure 2 shows the basic parameters of the coal samples from the middle and upper stratified layers and the coefficients of variation for the experimental results. By analyzing Figure 2, we can see that the coefficients of variation for the basic parameters (D, H, ρ, and V) of the coal samples from the middle and upper stratified layers were very small and generally did not exceed 5%; however, the coefficients of variation for the mechanical parameters (σ_c, E, E_{50}, and μ) were relatively large, above 18%.

The discreteness of the uniaxial compression peak strength is especially significant, and the coefficients of variation for the coal samples from the middle and upper stratified layers were 31.9% and 30.4%, respectively. The coefficients of variation for the elastic modulus, deformation modulus, and Poisson's ratio exceed 18.0%, which indicates the heterogeneous characteristics of the coal samples.

From Table 1, because of the crossing joint fractures distributed inside the coal sample and because the different directions and sizes of the joint cracks have varying degrees of influence on the deformation and strength of the coal

Table 1: Test results for coal samples subjected to uniaxial compression and step relaxation.

Position	Type	Coal number	D/mm	H/mm	ρ/kg·m^{-3}	V/m·s^{-1}	σ_c/MPa	E_T/GPa	E_{50}/GPa	μ
Middle	Conventional uniaxial	MZ1	49.4	103.7	1478	1865	33.39	4.44	3.62	0.31
		MZ2	49.5	102.9	1482	1780	19.58	4.01	2.71	0.36
		MZ3	49.4	100.4	1476	1770	31.97	3.95	2.93	0.26
		MZ4	49.5	98.0	1437	1795	26.46	4.15	3.05	0.33
	Stepwise relaxation	MZ5	49.5	99.3	1470	1770	12.10	2.40	1.53	0.21
		MZ6	49.5	101.1	1438	1893	27.31	3.81	3.40	0.31
Higher stratification	Conventional uniaxial	MS1	49.30	104.10	1470	1882	15.16	3.49	2.17	0.23
		MS2	49.50	100.60	1479	1729	15.28	3.30	1.95	0.36
		MS3	49.50	101.50	1461	1774	17.43	3.33	1.95	0.34
		MS4	49.70	102.40	1471	1965	7.97	2.16	1.64	0.19
	Stepwise creep	MS5	49.50	100.90	1469	1755	8.42	2.04	1.20	0.21
		MS6	49.50	98.20	1483	1839	15.50	3.65	2.71	0.30

Table 2: Test results of the uniaxial compression step relaxation tests.

Coal number	Progression	ε_1/10^{-3}	σ_s/MPa	(σ_r/σ_c)/%	t/s	$\Delta\sigma$/MPa	$\Delta\varepsilon_3$/10^{-3}
MZ4	①	4.26	13.07	49	603	0.18	0.00
	②	4.87	15.57	59	692	0.12	0.00
	③	5.51	18.11	68	573	0.11	0.04
	④	6.15	20.64	78	642	1.30	4.28
	⑤	7.26	23.44	89	555	1.10	2.37
	⑥	8.18	26.46	100	589	4.98	16.68
	⑦	9.04	21.00	79	128	5.47	3.40
MZ5	①	5.82	10.15	84	587	0.17	4.65
	②	6.62	11.74	94	590	0.90	12.85
	③	7.61	6.92	57	587	5.80	10.95
MZ6	①	3.11	10.43	38	577	0.07	0.00
	②	3.85	13.04	48	594	0.04	0.00
	③	4.50	15.56	57	572	0.12	0.00
	④	5.17	18.25	67	545	0.08	0.05
	⑤	5.79	20.85	76	549	0.11	0.04
	⑥	6.48	23.58	86	535	0.64	0.14

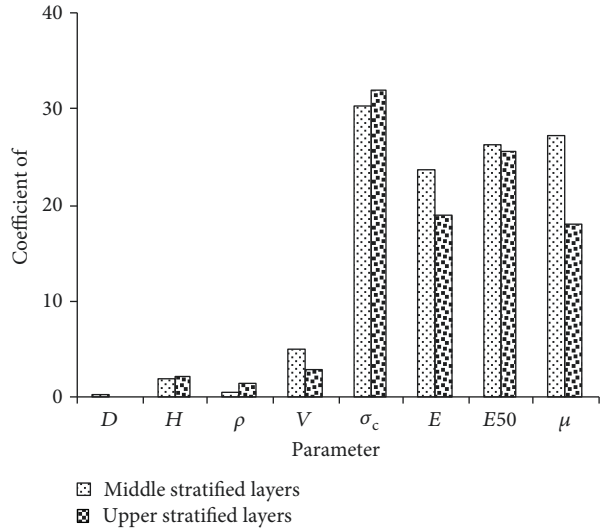

Figure 2: Basic parameters of coal samples and histograms of coefficients of variation obtained from the test results.

samples, the results of the uniaxial compression experiment were relatively discrete. Nonetheless, the average values of three samples can be used to characterize the mechanical characteristics of different loading modes. The peak strengths of the uniaxial compression tests for the six coal samples of the upper stratified layer ranged from 12.10 to 33.39 MPa, with an average peak strength of 25.13 MPa; these samples are hard coal. The peak strengths were relatively low for coal samples MZ2 and MZ5, which showed a relatively poor integrity and yielded values of 19.58 and 12.10 MPa, respectively. On the other hand, the peak strengths were relatively high for coal samples MZ1 and MZ3, which showed a relatively good integrity and yielded values of 33.39 and 31.97 MPa, respectively. The highest and lowest peak strengths showed two- to three-fold differences. The peak strengths of the conventional uniaxial compression tests ranged from 19.58 to 33.39 MPa, with an average of 28.31 MPa; the elastic modulus ranged from 3.95 to 4.44 GPa, with an average of 4.13 MPa; the deformation modulus ranged from 2.71 to 3.62 GPa, with an average of 3.09 MPa; and Poisson's ratios ranged from 0.26 to 0.36, with an average of 0.31. The peak strengths of the uniaxial staged relaxation tests ranged from 12.10 to 27.31 MPa, with an average of 21.97 MPa; the elastic modulus ranged from 2.40 to 3.81 GPa, with an average of 3.45 MPa; the deformation modulus ranged from 1.53 to 3.40 GPa, with an average of 2.66 MPa; and Poisson's ratios ranged from 0.21 to 0.30, with an average of 0.28. In comparison with the conventional uniaxial experiment, the peak strength, elastic modulus, deformation modulus, and Poisson's ratio obtained in the staged relaxation experiment declined by 22.45%, 16.5%, 13.82%, and 8.60%, respectively.

In comparison with the coal sample from the upper stratified layer, the peak strengths of the coal samples from the stratified layer in the middle were relatively low, as expected. The peak strengths of the uniaxial compression test for the

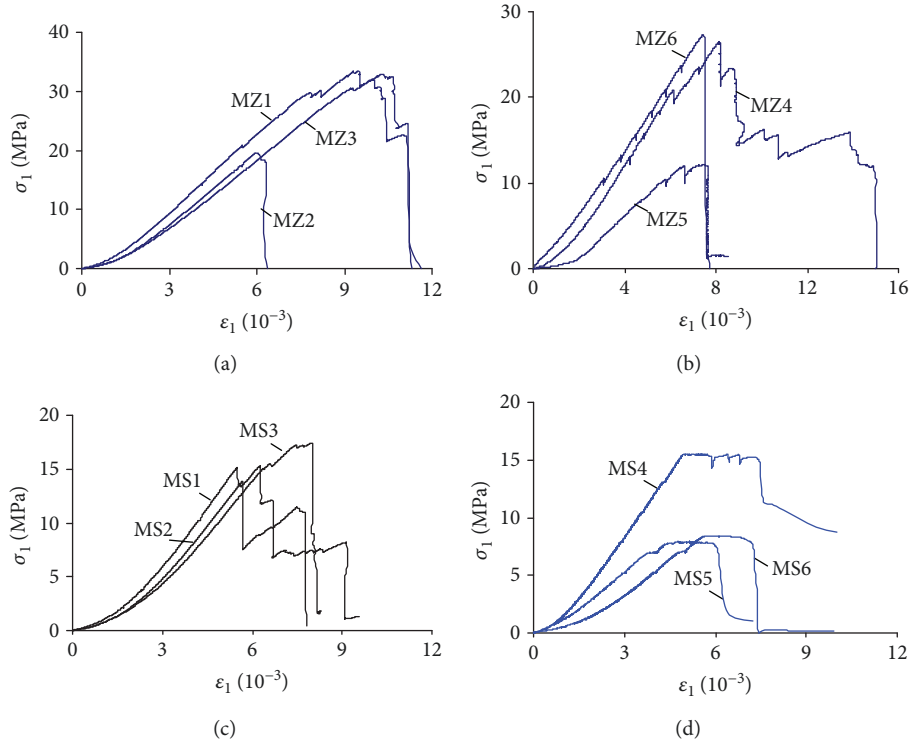

Figure 3: Stress-strain curves of the uniaxial compression and step loading tests.

six coal samples ranged from 7.97 to 17.43 MPa, with an average of 13.29 MPa, which signifies medium-hard coal. The peak strengths of the uniaxial compression tests for the three coal samples ranged from 15.16 to 17.43 MPa, with an average of 16.96 MPa; the elastic modulus ranged from 3.30 to 3.49 GPa, with an average of 3.37 MPa; the deformation modulus ranged from 1.95 to 2.17 GPa, with an average of 2.02 MPa; and Poisson's ratios ranged from 0.23 to 0.36, with an average of 0.31. The peak strengths of the staged creep tests ranged from 7.97 to 15.50 MPa, with an average of 10.63 MPa; the elastic modulus ranged from 2.04 to 3.65 GPa, with an average of 2.62 MPa; the deformation modulus ranged from 1.20 to 2.71 GPa, with an average of 1.85 MPa; and Poisson's ratios ranged from 0.19 to 0.30, with an average of 0.23. In comparison with the conventional uniaxial experiment, the peak strengths, elastic modulus, deformation modulus, and Poisson's ratios obtained for the loading of staged creep experiments declined by 33.38%, 22.40%, 8.57%, and 24.73%, respectively.

According to the analysis presented above, we can see that the mechanical parameters of coal samples not only depend on factors such as the size and distribution direction of joint cracks inside them but also they are related to the loading type and mode. The mechanical parameters obtained in the uniaxial compression experiment are clearly higher than the values of the staged relaxation (creep) loading experiment, indicating that the mechanical parameters of the coal samples show the characteristics of time-delayed progressive failure.

Figure 3 shows the whole-process stress-strain curve of the uniaxial compression and staged relaxation (creep) experiments for three coal samples. We can see from Figure 3 that, under the three loading types, there is no clear difference in the stress-strain curves before the peak strength was applied, and the deformation failure after the peak is related to the loading type. The coal sample goes through the stages of compaction, elasticity, yield, and failure during the entire compression process. There is staged destruction for a portion of the coal samples from the middle (upper) stratified layer after the peak uniaxial compression is reached, and the stress curve exhibits a stepwise decline, as shown by coal samples MZ1 and MZ3 in Figure 3(a) and MS1 and MS2 in Figure 3(c). After the peak, there are two to three periods of rapid stress decline. After the first stress decline, the bearing force continues to increase as the axial compression deformation increases, and then, the stress decreases again, showing the brittleness characteristics of the coal samples.

Figure 3(b) shows the whole-process stress-strain curve of the uniaxial staged relaxation loading experiment for the coal samples from the stratified layer in the middle. During the relaxation period, characteristics of region-wise stress decline were observed, and the value of these stress declines is related to the relaxation stress level. The higher the relaxation stress level is, the more pronounced the stress decrease becomes. Figure 3(d) shows that, in the uniaxial staged creep experiment on the coal samples, coal samples MS4, MS5, and MS6 were sequentially loaded on levels 2, 3, and 4. The creep loading stress level was relatively low for the first three levels for coal sample MS6. When the loading stress of coal sample MS6 was lower than its yield strength, the internal damage of the coal sample was very small during the creep period, and the axial strain of the coal sample was not clear, which demonstrates characteristics that are essentially the same as those of conventional uniaxial compression deformation. That is,

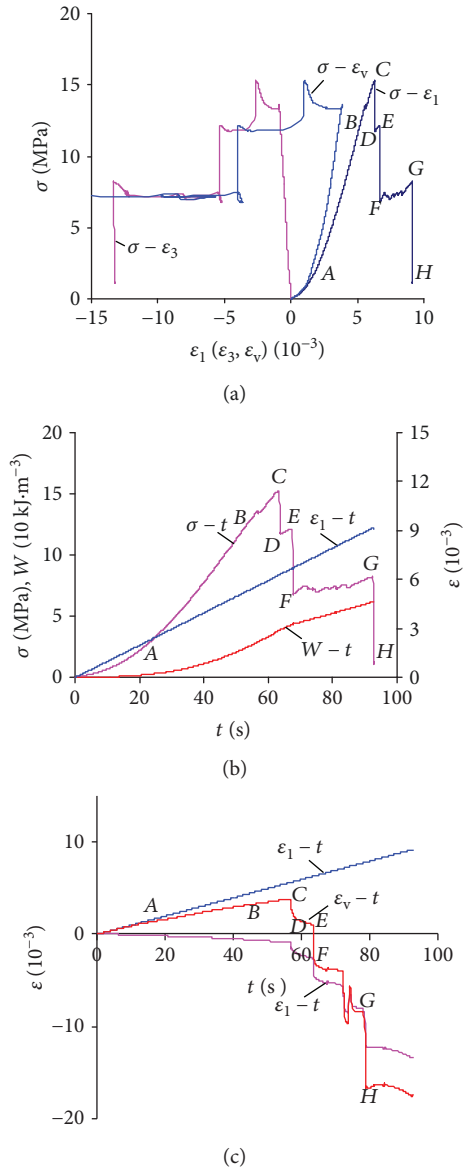

Figure 4: Stress (strain, energy) versus time curves for MS2 under uniaxial compression.

the stress-strain curve was smooth without fluctuations. During the constant loading process on level 4, the loading stress level exceeded the yield strength of the coal sample. During the creep period, as the creep time increased, the axial deformation of the coal sample continued to increase, and the stress slightly fluctuated. When the axial deformation reaches the peak strain, the coal samples eventually fail. There was no clear peak point for coal samples MS5, MS6, and MS4, which all showed a yield plateau in their curves and whose stress values rapidly declined after the peak.

3.2. Results of the Uniaxial Compression Experiment. Before we conducted the uniaxial staged relaxation (creep) experiment, we first conducted the conventional uniaxial compression experiment, which was convenient for reasonably determining the relaxation (creep) stress levels and grade of the samples. The uniaxial staged relaxation (creep) loading experiment can proceed smoothly and is also convenient for comparing mechanical parameters under the three loading types considered, thus obtaining the rules behind the characteristics of time-delayed progressive failure for additional coal samples. Figure 4 shows the whole-process stress (strain, energy) time curves for the uniaxial compression of coal sample MS2 (because of space limitations, the results for the other coal samples are not shown in this paper).

It should be noted that the deformation and failure energy of coal samples during loading can be divided into stress-strain curves and strain axes:

$$U = \int_0^{\varepsilon_1} \sigma_1 d\varepsilon_1. \tag{1}$$

According to the definition of the definite integral shown in equation (1), the sum of the areas of small trapezoidal strips can be carried out using the stress-strain curve:

$$U = \sum_{i=0}^{n} \int \frac{1}{2} \left(\sigma_1^i + \sigma_1^{i+1}\right) \left(\varepsilon_1^{i+1} - \varepsilon_1^i\right). \tag{2}$$

In equation (2), n is the calculated sample number of the axial stress-strain curve at any time during the test, i is the sampling point, and σ and ε are the stress and the strain at the sampling point, respectively.

As shown in Figure 4, during conventional uniaxial compression and under the condition of setting the displacement control to apply a continuous load, the axial strain of coal samples exhibited a linear relationship with time. The accumulated energy during the loading process continued to increase, as shown in Figure 4(b). During the loading process, owing to the influence of primitive joint fractures inside the coal samples, the primitive joint cracks that occurred during the initial stage of the loading process gradually closed, and the stress-strain curve became concave and gradually steeper. The enhancement of the axial deformation was relatively fast, the increase of the circumferential deformation was slow, and the volumetric strain gradually increased. During this stage (OA), the accumulated energy of the coal samples was relatively low, and part of the accumulated energy was consumed by the closure of cracks. As the axial stress increased into the elastic stage, the axial stress and the axial and circumferential strains exhibit a roughly linear relationship, showing the elastic characteristics of the coal samples. The coal samples stored a significant amount of elastic energy during this stage (AB). When the axial load reached 70% of the peak load, the coal sample entered the yield stage (BC). As the axial load increased, the materials with a relatively low strength inside the coal sample were the first to yield and fail, and then, the primitive fissures slipped. New microcracks continuously appeared, evolved, developed, and converged, making the stress-strain curve deviate from a straight line and gradually decelerate. The velocity of the axial strain remained unchanged. At this stage, high-strength materials will bear an even higher stress and gradually yield, get damaged, and fail. The circumferential strain accelerated as the stress increased, reaching approximately 90% of the peak strength.

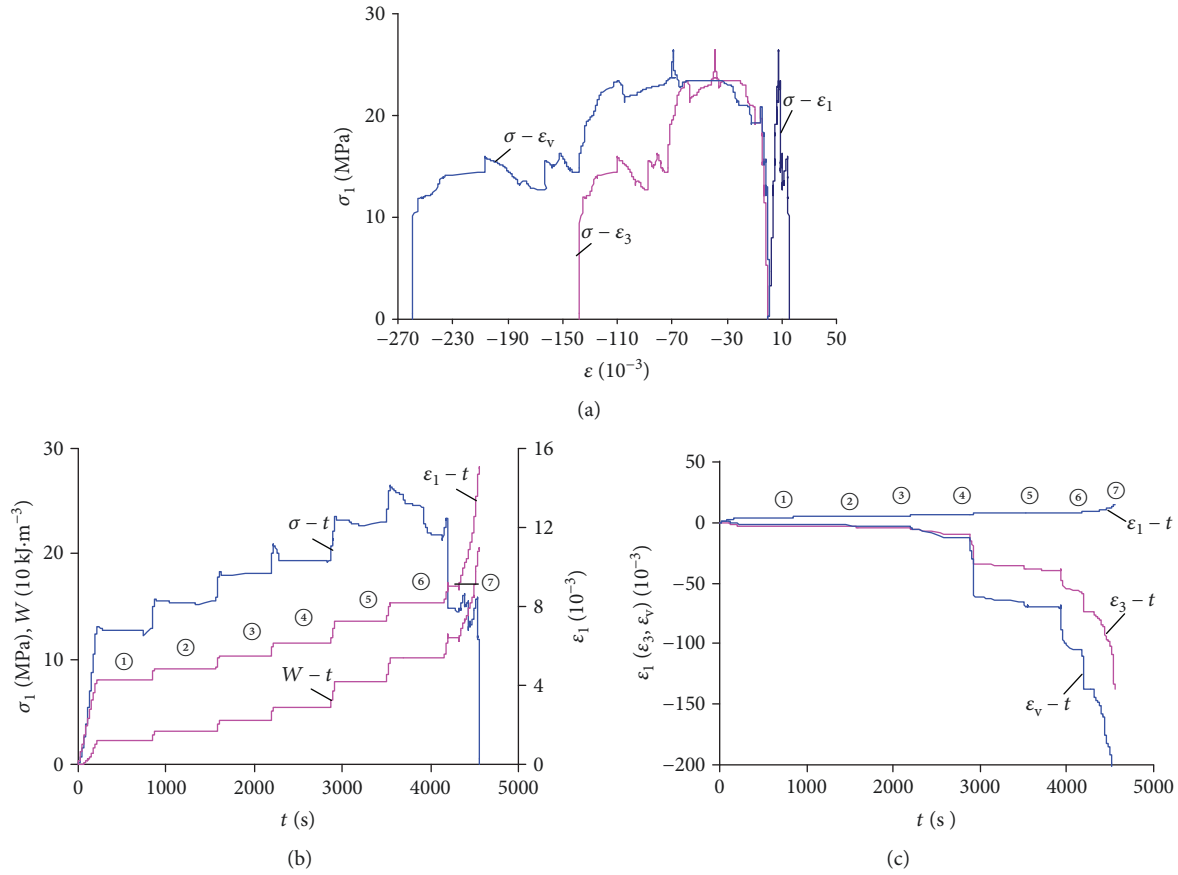

Figure 5: Complete stress (strain, energy) versus time curves for the uniaxial compression step relaxation of coal sample MZ4.

There was a surge in the circumferential strain, indicating that the volumetric strain of the coal samples changed from increasing to decreasing. To put it differently, the volume of the coal samples began to increase. This phenomenon of volume expansion is a warning sign of coal sample failure. The coal sample is locally destroyed, while the main body structure can still bear a load. Once the stress reaches its peak strength, the macroscopic fractures cause the destruction of the load-bearing skeleton. The carrying capacity of the macroscopic crack slips decline, and the accumulated energy of the coal samples prior to the peak is released after the peak, forcing the coal samples to gradually lose their stability and fail.

Figure 4 shows that there was a rapid staged stress decline after the peak in coal sample MS2. Upon reaching the peak strength, the first rapid stress decline ($C \rightarrow D$) occurred instantaneously, and longitudinal cracks appeared locally inside the coal sample. The circumferential strain slightly increased, but the volume of the coal sample did not exceed the original volume. As the axial compression strain increased, the carrying capacity increased with small amplitude changes until point E, at which the second fast stress decline ($E \rightarrow F$) occurred. The longitudinal cracks penetrated to form macroscopic cracks. The circumferential strain rapidly increased and the volumetric strain rapidly expanded, causing a volume expansion. Then, as the axial deformation continued to increase and the carrying capacity increased with small fluctuations until point G, the third rapid stress decline ($G \rightarrow H$) occurred. At this stage, the circumferential strain of the coal samples multiplied, and their volume rapidly expanded and longitudinally transversed the fractures. As the coal body is compressed to break, the coal sample loses its stability and fails. This indicates that upon uniaxial compression of the coal samples, internal damage to the coal samples is gradually generated; they exhibited a tensional staged fracture, lost their stability, and failed after the peak, showing the brittleness characteristic of the coal samples.

3.3. Results of the Uniaxial Staged Relaxation Experiment. Table 2 shows the results of the uniaxial compression staged relaxation experiment for three coal samples from the stratified layers in the middle. In this table, σ_s is the relaxation stress, σ_s/σ_c is the relaxation stress ratio (namely, the ratio between relaxation stress and peak strength), t is the duration of relaxation, $\Delta\sigma$ is the magnitude of the stress decline during the relaxation period, and ε_1 and $\Delta\varepsilon_3$ are the amplitudes of the increases in the axial and circumferential strains during the staged relaxation period, respectively. The strength of coal samples MZ4 and MZ6 was relatively high; there were five to six relaxations before the peak and one relaxation after the peak. The strength of coal sample MZ5 was clearly low, and there were two relaxations before the peak and one relaxation after the peak. Figure 5 shows the whole-process stress (strain, energy) versus time curve of the uniaxial compression staged relaxation experiment for coal sample MZ4 (because of space limitations, the results for coal samples MZ5 and MZ6 are not shown).

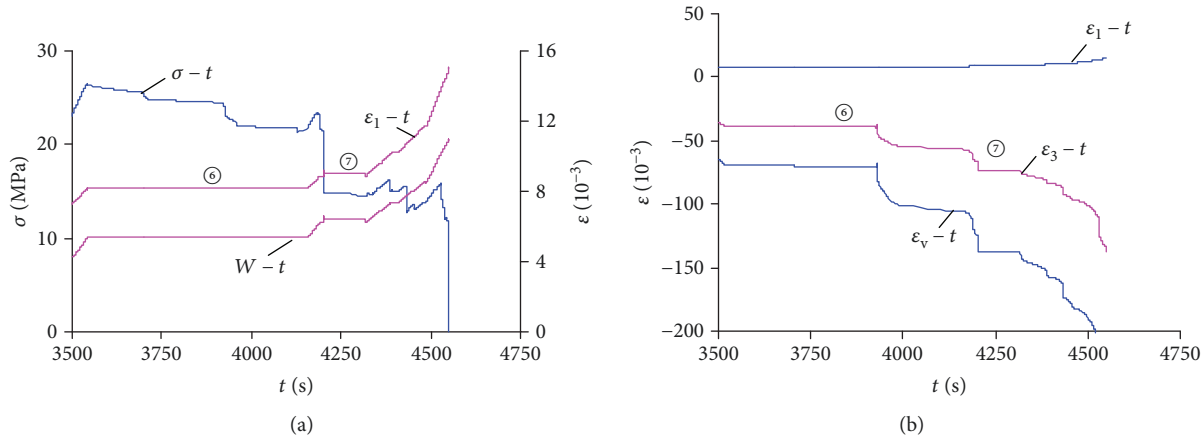

Figure 6: Stress (strain, energy) versus time curves for the sixth and seventh state relaxation tests.

Our analysis indicates that the characteristics of the whole-process stress-strain curve shown in Figure 5 for the uniaxial compression staged relaxation of coal sample MZ4 are roughly the same as those of the conventional uniaxial compression; there is no clear difference. The variations in the stress (strain and energy) versus time curve during the staged relaxation loading process exhibit a clear difference, and the strain and energy versus time curve exhibits a stepwise increase before the loading stress reaches its peak strength. That is, the axial strain remained unchanged during the relaxation period, whereas the circumferential strain and axial stress exhibited different features over time. The test machine did not operate on the samples during the relaxation period.

During the initial loading stage, the primitive fissures of the coal samples were closed. The axial strain was relatively large, and the circumferential (volume) strain was relatively small. When level 1 was loaded with 13.07 MPa (with a stress ratio of 49%) for a 603 s period, the magnitude of the stress decline was 0.18 MPa and the circumferential strain remained unchanged; when level 2 was loaded with 15.57 MPa (with a stress ratio of 59%) for a 692 s period, the magnitude of the stress decline was 0.12 MPa and the circumferential strain remained unchanged; when level 3 was loaded with 18.11 MPa (with a stress ratio of 68%) for a 573 s period, the magnitude of the stress decline was 0.11 MPa and the circumferential strain slightly increased. Therefore, the relaxation stress ratio was lower than 68. When the sample was loaded with 18.11 MPa (with a stress ratio of %), the magnitude of the stress decline did not exceed 0.20 MPa and the magnitude of the axial strain increased by 29.3%. The circumferential strain remained essentially unchanged, which indicates that it had reached the elastic stable state inside the coal sample and that no damage was done inside the coal sample during the first three relaxation periods.

When level 4 was loaded with 20.64 MPa (with a stress ratio of 78%) for a 642 s period, the stress declined relatively fast in the first 33 s and then remained unchanged. The magnitude of the stress decline was 1.30 MPa, and the magnitude of the circumferential strain increase was 4.28×10^{-3}, which indicates that the relaxation stress ratio was higher than 78%. Although the axial deformation no longer increased, the test machine did not operate on the coal samples during relaxation, and the microcracks inside the coal sample gradually germinated, evolved, and developed by relying on the energy accumulated by the coal sample during the preceding period. When level 5 was loaded with 23.44 MPa (with a stress ratio of 89.0%) for a 555 s period, the stress declined relatively fast during the first 200 s and then remained unchanged. The total magnitude of the decline was 1.10 MPa, and the total magnitude of the circumferential strain increase was 2.37×10^{-3}.

When level 6 was loaded with 20.64 MPa (with a stress ratio of 100%) for the relaxation test, a mutation phenomenon occurred in the stress-strain curve of the coal sample. For the sake of convenience, we zoomed in to show the stress (strain, energy) versus time curve during the relaxation period on levels 6 and 7, as shown in Figure 6. We can see from Figure 6 that during the 589 s period for the relaxation of level 6, the stress showed the occurrence of a phenomenon consisting of multiple declines, and the magnitude of the stress decline reached 4.98 MPa. The circumferential strain rapidly increased, and the amplitude of the increase reached 18.67×10^{-3}. It can be seen that when the relaxation stress was higher than the peak strength of the coal sample, even though the test machine did not supply energy during the relaxation period, the elastic energy accumulated by the high-strength materials inside the coal sample could be continuously released, forcing the low-strength materials inside the coal sample to continuously yield and fail. The microcracks inside the coal sample constantly evolved, developed, and converged as the relaxation period went on, eventually forming macroscopic cracks that reduced the carrying capacity of the coal sample. When the stress decreased to a peak value of 21.0 MPa (with a stress ratio of 79%), we conducted relaxation on level 7 after the peak. During a 128 s period, the stress of the main bearing skeleton inside the coal sample constantly adjusted and exhibited a steady decline with fluctuations; the magnitude of the stress decline was 5.47 MPa. The axial strain rapidly increased, and then, the circumferential and volumetric strains rapidly increased. The coal sample continuously shed fragments, eventually lost its stability, and failed; the carrying capacity rapidly declined to zero.

Table 3: Parameters of coal samples under step loading.

Coal number	Progression	σ_r/MPa	(σ_r/σ_c)/%	t/s	$\Delta\varepsilon_1/10^{-3}$	$\Delta\varepsilon_3/10^{-3}$	Σt/s
MS4	①	5.21	65	568	0.29	0.03	675
	②	6.96	87	1074	1.08	0.18	1831
MS5	①	5.25	62	592	0.02	0.00	700
	②	7.00	83	856	0.23	0.21	1600
	③	8.42	100	25	0.32	0.39	1654
MS6	①	7.90	51	583	0.10	0.10	746
	②	10.46	67	598	0.08	0.09	1404
	③	13.00	84	630	0.09	0.22	2094
	④	15.50	100	205	0.25	2.06	2362

The analysis presented above indicates that the deformation and strength of coal samples during uniaxial staged relaxation experiments are closely related to the relaxation stress ratio (time). The relaxation stress ratio on level 4 of coal sample MZ4 was 78%, the relaxation stress ratio on level 1 of coal sample MZ5 was 84%, and the relaxation stress ratio on level 5 of coal sample MZ6 was 76%. Thus, the time characteristics of relaxation become apparent. To put it differently, the stress decline of the coal sample is evident when the circumferential and volumetric strains begin to increase.

3.4. Results of the Uniaxial Staged Creep Experiment. Table 3 shows the results of the uniaxial staged creep experiment for the coal samples from the upper stratified layer. In this table, σ_r is the creep stress, σ_r/σ_c is the creep stress ratio (i.e., the ratio between creep and peak strengths), t is the creep time, Σt is the cumulative time of the experiment, and $\Delta\varepsilon_1$ and $\Delta\varepsilon_3$ are the increments of the axial and circumferential strains during the staged creep period, respectively. We can see from Tables 1 and 3 that the compression strength of coal sample MS5 was clearly low. After the creep on level 2, coal sample MS4 was again destroyed during the loading process, and the peak strength was 7.97 MPa. The compression strength of coal sample MS6 was relatively high. Coal sample MS6 lost its stability and failed during the creep process on level 4, and the peak strength was 15.50 MPa. The compression strength of coal sample MS5 was between these two, and its peak strength was 8.42 MPa. Coal sample MS5 lost its stability and failed during the creep process on level 3.

Figure 7 shows the whole-process stress (strain, energy) versus time curves of the uniaxial staged creep experiment for coal sample MS6, which was taken from the upper stratified layer (because of space limitations, the results for coal samples MS4 and MS5 are not shown). Compared with the relaxation experiment shown in Figure 5, the uniaxial staged creep experiment was different. Upon uniaxial staged creep, the axial stress of the coal sample exhibited a roughly stepwise increase with time. During the staged creep period, the axial stress remained constant. The axial strain (energy) continued to increase, and the test machine constantly supplied energy to the coal samples. From the results of the uniaxial staged creep experiments on the coal samples, it can be seen that the characteristics of the axial strain (energy) variations over time are clearly different from those of the uniaxial compression.

When the sample was loaded with 7.90 MPa (with a stress ratio of 51%) on level 1 while maintaining stress constant, the axial (circumferential) strain did not change considerably for a 583 s period, and the magnitude of the enhancement was 0.1×10^3. When level 2 was loaded with 10.46 MPa (with a stress ratio of 67%) and while maintaining stress constant for a 598 s period, the axial and circumferential strains were roughly equal, and the magnitudes of the enhancements were 0.08×10^3 and 0.09×10^3, respectively. When level 3 was loaded with 13.00 MPa (with a stress ratio of 84%) while maintaining axial stress constant for a 630 s period, the increase of the axial strain was slow whereas the increase of the circumferential strain was fast, with the magnitudes of the enhancements being 0.09×10^3 and 0.22×10^3, respectively. The volumetric strain began to decrease, which means that the interior of the coal sample was constantly damaged that and microcracks gradually germinated, evolved, developed, and converged. When level 4 was loaded with 15.50 MPa (with a stress ratio of 100%), the coal sample gradually lost its stability and failed. For ease of description, the stress (strain, energy) versus time curve during the creep period on level 4 was expanded and is shown in Figure 8.

By analyzing Figure 8, we can see that when the staged creep stress approached its peak strength, even though the axial stress of the coal sample remained essentially constant, the increase of the axial strain was slow. However, the circumferential strain rapidly increased, and its value was much larger than that of the axial strain. The volume rapidly expanded, and the coal sample was suddenly destroyed after 205 s. It is clear from Figure 8(a) that the strain-time curve is similar to the uniaxial compression creep experiment curve for normal rock, and thus, we can divide this creep curve into three stages, namely, instantaneous creep (I), steady creep (II), and accelerated creep (III). However, there are still essential differences between the uniaxial staged creep and conventional uniaxial creep experiments. The primary differences are as follows: (1) the stress in the conventional creep experiments was higher than the long-time strength and lower than the instantaneous peak strength, whereas in the uniaxial staged loading experiments, the loading stress level on the last level was close to the uniaxial compression instantaneous peak strength of the coal samples; (2) the duration of the conventional creep experiments was relatively long, while the duration of the staged creep experiments was relatively short; and (3) when the samples were close to failure, the form of the time versus strain curves during the acceleration stage was also different, and the deformation velocity at the acceleration stage was relatively slow in the conventional creep experiments and relatively fast for the staged creep experiments. This is because the destruction of rocks during conventional creep experiments is caused by the slow slipping dislocation of crystals, while the destruction of the coal samples during uniaxial staged creep experiments is primarily caused by the rapid opening and breaking of vertical cracks.

In summary, during the relaxation (creep) experiments, when the relaxation (creep) stress ratio was lower than

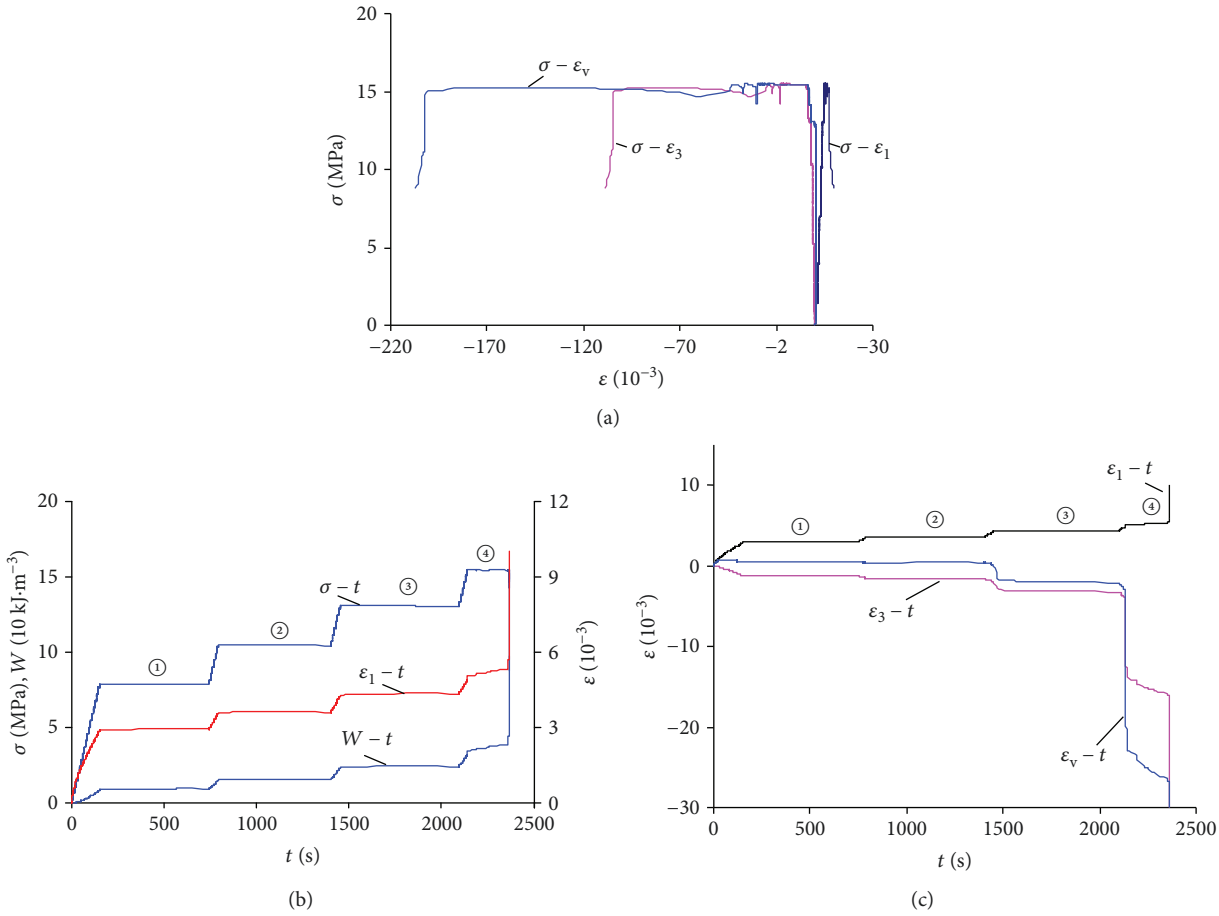

Figure 7: Complete stress (strain, energy) versus time curves for the step loading tests.

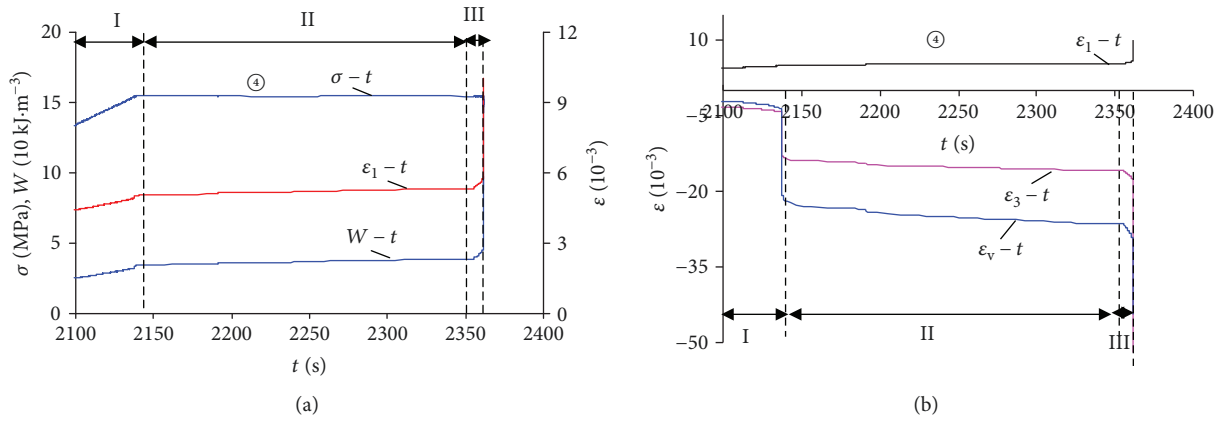

Figure 8: Stress (strain, energy) versus time curves for the step loading tests.

70%, the characteristics of the relaxation (creep) effects are not clear; when the relaxation (creep) stress ratio was higher than 70%, even though the axial strain (stress) remained constant during relaxation, the energy accumulated by the materials with a relatively high strength inside the coal samples could cause the materials with a relatively low strength to get gradually damaged and fail as time went on and cause new microcracks to constantly evolve, develop, and converge. High-strength materials can bear a higher stress and gradually tend to fail, and the carrying capacity of coal samples will constantly decline as relaxation time passes. During the creep period, the axial and circumferential deformations of coal samples gradually increase, and their volume constantly expands. Even when the stress is lower than the peak strength, maintaining a constant strain (stress) over a long period of time can also make the coal body yield and fail.

The higher the relaxation (creep) stress level is, the shorter the duration of damage becomes. Conversely, the duration of damage becomes longer when the stress level is lower. Therefore, for a fully mechanized mining face, by increasing the resistance of the support, timely moving the support after coal cutting, reducing the stress of the coal body in front of the working face, and shortening the exposure time of the coal wall, we can effectively prevent the occurrence of coal wall spalling accidents.

3.5. Failure Characteristics. The conventional uniaxial and uniaxial staged relaxation (creep) failure of coal samples from the middle and upper stratified layer is shown in Figure 9; we also provide sketches of the cracks.

It can be seen from Figure 9 that the coal failures in the conventional uniaxial experiments were relatively simple and had an evident tension-shear dual fracture surface. The number of cracks was relatively small and the fracture plane was roughly parallel to the loading direction, such as fractured surface A of coal sample MZ2. The majority of the coal samples exhibited one or several dominant cracks, which expanded and initialized the cracking process. When the secondary cracks could not fully expand, the entire coal sample was broken into many blocks. While the coal samples showed tensional cracks, these were also accompanied by shear-type slip surfaces, such as the shear-type slip surfaces B and C of coal samples MZ1 and MZ3 from the stratified layer in the middle, as shown in Figure 9(a). Figure 9(c) shows the two tensile cracks, A and B, which first appeared in coal sample MS1 from the upper stratified layer. As the stress increased, a staged fracture appears in the middle of a thin sheet to form the transversal crack C, which is in agreement with the characteristics of the multiple stress decreases on the stress-strain curve after the peak shown in Figure 2 for coal sample MS1. Coal samples MS2 and MS4 showed two shear-type slip surfaces and eventually exhibited X- and V-type failure forms.

The lateral expansion of the coal samples was somewhat evident, such as in coal block D of coal sample MZ4 and coal block F of coal sample MZ5 from the stratified layer in the middle, as shown in Figure 9(b). Figure 9(d) shows that coal samples MS4 and MS6 had many longitudinal cracks parallel to the loading direction and that shear-type secondary cracks were generated at many locations.

4. Discussion

As the axial load increased, the materials with a relatively low strength inside the coal sample were the first to yield and fail, and then, the primitive fissures slipped. New microcracks continuously appeared, evolved, developed, and converged, making the stress-strain curve deviate from a straight line and gradually decelerate. The velocity of the axial strain remained unchanged. At this stage, high-strength materials will bear an even higher stress and gradually yield, get damaged, and fail. The shear cracks initiate followed by a large and abrupt compressive strain jump and then quickly propagate in an unstable manner resulting in the failure of specimens.

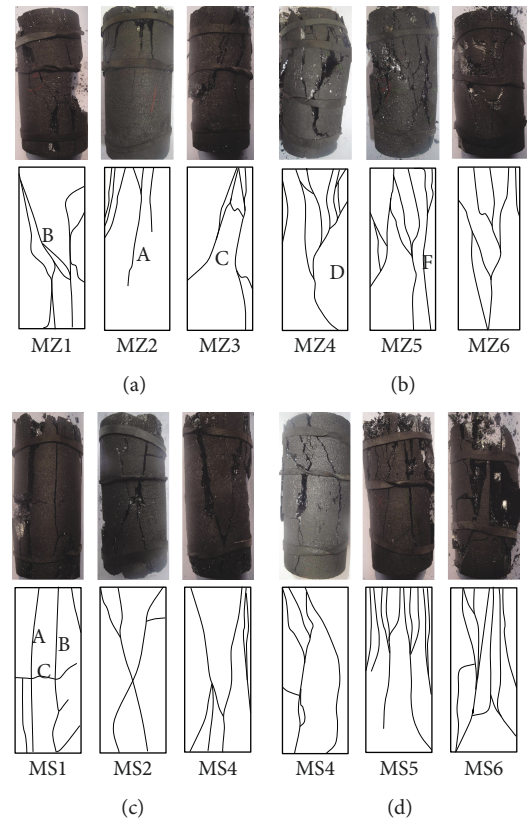

Figure 9: Failure modes of coal samples for the uniaxial compression and step loading tests.

Because of the crossing joint fractures distributed inside the coal sample and because the different directions and sizes of the joint cracks have varying degrees of influence on the deformation and strength of the coal samples, the results of the uniaxial compression experiment were relatively discrete. Nonetheless, the average values of three samples can be used to characterize the mechanical characteristics of different loading modes.

Although the axial deformation no longer increased, the test machine did not operate on the coal samples during relaxation, and the microcracks inside the coal sample gradually germinated, evolved, and developed by relying on the energy accumulated by the coal sample during the preceding period. When the relaxation stress ratio was higher than 70, the time characteristics of relaxation become apparent. To put it differently, the stress decline of the coal sample is evident when the circumferential and volumetric strains begin to increase. Yang et al. conducted a uniaxial compression time-delayed failure experiment on marble and found that the circumferential strain upon the occurrence of marble time-delayed failure is clearly larger than the axial strain [1]. The analysis presented above indicates that the deformation and strength of the coal samples during uniaxial staged relaxation experiments are closely related to the relaxation stress ratio (time).

Compared with the conventional uniaxial experiments, in the staged relaxation (creep) experiments, the microfissures of the coal samples were fully developed and the failure

forms were relatively complex because the duration of the loading process was relatively long. The cracks primarily expanded along the loading direction and then broke into many relatively thin sheets and sheet clastics. This is because in the staged relaxation (creep) experiments, under the action of stress below the peak strength, the microcracks inside the coal sample had sufficient time to slowly expand. Eventually, in addition to forming one or several dominant macrocracks, expansion will also form many secondary cracks, which split the entire coal sample into many thin-sheet clastics that gradually collapse and shed, and thus, the number of cracks increases. The staged relaxation (creep) experiments of the coal samples demonstrated failure characteristics that are extremely similar to the failure characteristics of coal wall spalling on the working faces of coal mines.

5. Conclusions

(1) The stress-strain curves before the peak value for coal samples under conventional uniaxial compression and graded relaxation (creep) loading are not different from each other, and both show stages of compaction, elasticity, yield, and failure. Local stress drops appear during stage relaxation, and there is no clear peak point in the graded creep tests, in which a yield plateau appears

(2) The mechanical parameters obtained in the conventional uniaxial compression tests are clearly higher than those obtained in the uniaxial compression staged relaxation tests, which shows that the mechanical parameters of coal samples are time-sensitive

(3) When the stress ratio was lower than 70, the stress relaxation (creep) was not evident. When the relaxation (creep) stress ratio was higher than 70, the displacement (stress) remained constant during relaxation (creep). As the relaxation (creep) time passed, the internal microcracks in the coal continued to evolve, develop, and converge. The higher the stress level of relaxation (creep) was, the shorter the damage duration was and the longer the damage duration was. In fully mechanized coal faces, coal-wall- and cover-related accidents can be effectively prevented by raising the supporting resistance and moving the frame support in time after cutting coal, thus reducing the stress of the coal body in the face front and shortening the time of coal wall exposure

(4) Conventional uniaxial compression failure is simple and clearly presents tension-shear double-fracture surfaces. The failure forms of the coal samples were more complicated during the stage relaxation (creep) tests. The entire coal samples were divided into many thin fragments via collapsing and shedding, and the number of cracks consequently increased, showing evident lateral expansion characteristics. These were very similar to the characteristics of the delayed failure of coal walls and cover in high mining faces

Data Availability

The data used to support the findings of this study are included within the supplementary information files.

Conflicts of Interest

The authors declare that they have no conflicts of interest.

Acknowledgments

The research was supported by the Natural Science Foundation of China (no. U1504529).

Supplementary Materials

We conducted uniaxial compression and uniaxial staged relaxation (creep) experiments on coal samples from the upper (middle) stratified layer of a coalbed in the Zhaogu no. 2 mine. The coal samples from the upper stratified layer were numbered as MS1–MS6, and the coal samples from the middle stratified layer were numbered as MZ1–MZ6. (1) According to the loading type applied, the uniaxial compression experiments can be divided into conventional uniaxial compression, uniaxial compression stepwise relaxation, and uniaxial compression stepwise creep. There are twelve coal samples and twelve experimental data files with prefix titled "conventional uniaxial," "stepwise relaxation," and "stepwise creep" as supplementary material to our manuscript, respectively. (2) Table 1 shows the results of the conventional uniaxial and staged relaxation (creep) experiments for the coal samples, respectively. And D, H, ρ, V, σ_c, E_T, E_{50}, and μ are the diameter, height, natural density, longitudinal wave velocity, uniaxial peak strength (relaxation, creep), modulus of elasticity, deformation modulus, and Poisson's ratio of the coal sample, respectively. (3) The experiments were conducted on an RMT-150B electrohydraulic servo rock test system. It automatically collected the load and deformation information during the experimental process. Each experimental data file consists of the load and deformation information, namely, time, axial force, axial deformation, lateral deformation, axial stress, axial strain, lateral strain, volumetric strain, time, and energy. The figures (Figures 3~8) in the manuscript were displayed in real time to obtain the whole-process stress-strain curve of the uniaxial compression staged creep (relaxation), stress (strain, energy) versus time curves and complete stress (strain, energy) versus time curves of the coal samples. *(Supplementary Materials)*

References

[1] Y. Yang, H. Zhou, C. Zhang, K. Zhang, and F. Yan, "Experimental investigation on time-lag failure properties of marble under uniaxial compressive test," *Rock and Soil Mechanics*, vol. 32, no. 9, pp. 2714–2720, 2011.

[2] T. Feng, W. Wang, and C. Pan, "Load relaxation tests of rock and research on two types of rockburst," *Journal of Xiangtan Mining Industry*, vol. 15, no. 1, pp. 27–31, 2000.

[3] L. Tang and C. Pan, "Experiment study on properties of stress relaxation of rock under deformation at peak load," *Rock and Soil Mechanics*, vol. 24, no. 6, pp. 940–942, 2003.

[4] Y. Li, "Creep and relaxation of four kinds of rocks under uniaxial compression tests," *Chinese Journal of Rock Mechanics and Engineering*, vol. 14, no. 1, pp. 39–47, 1995.

[5] C. Yang, S. Bai, and Y. Wu, "Effect of stress level and loading path on time dependent properties of salt rock," *Chinese Journal of Rock Mechanics and Engineering*, vol. 19, no. 3, pp. 270–275, 2000.

[6] H. Tian, W. Chen, D. Yang, and F. Dai, "Relaxation behavior of argillaceous sandstone under high confining pressure," *International Journal of Rock Mechanics and Mining Sciences*, vol. 88, pp. 151–156, 2016.

[7] C. Paraskevopoulou, M. Perras, M. Diederichs et al., "The three stages of stress relaxation-observations for the time-dependent behaviour of brittle rocks based on laboratory testing," *Engineering Geology*, vol. 216, pp. 56–75, 2017.

[8] P. Xu, T. Yang, C. Xu, and H. Zhou, "Creep characteristics and long-term stability of rock mass in ship lock high slope of the Three Gorges Project," *Chinese Journal of Rock Mechanics and Engineering*, vol. 21, no. 2, pp. 163–168, 2002.

[9] N. Liu, C. Zhang, and W. Chu, "Experimental research on time-dependent behavior of crack propagation in Jinping deep marble," *Rock and Soil Mechanics*, vol. 33, no. 8, pp. 2437–2450, 2012.

[10] H. Yu, Y. Li, and H. Liu, "Comparative study of conventional mechanical, creep and stress relaxation properties of silty mudstone under triaxial compression," *Chinese Journal of Rock Mechanics and Engineering*, vol. 31, no. 1, pp. 60–70, 2012.

[11] G. Han, S. Wang, X. Zhang, Y. Wang, G. Zhao, and C. Ma, "Study of creep properties of thinly laminated rock under step loading," *Chinese Journal of Rock Mechanics and Engineering*, vol. 29, no. 11, pp. 2239–2247, 2010.

[12] Y. Li, "Experimental study of creep properties of silty mudstone under triaxial compression," *Journal of Sichuan University(Engineering Science Edition)*, vol. 44, Supplement 1, pp. 14–19, 2012.

[13] C. Zhang, N. Liu, H. C. Zhu, W. Chu, and J. Y. Wu, "Time-dependent behavior of crack propagation and evaluation of control effect of jinping deep marble," *Chinese Journal of Rock Mechanics and Engineering*, vol. 32, no. 10, pp. 1964–1972, 2013.

[14] R. Wang, Z. Zhuo, H. W. Zhou, and J. F. Liu, "A fractal derivative constitutive model for three stages in granite creep," *Results in Physics*, vol. 7, pp. 2632–2638, 2017.

[15] O. Hamza and R. Stace, "Creep properties of intact and fractured muddy siltstone," *International Journal of Rock Mechanics and Mining Sciences*, vol. 106, pp. 109–116, 2018.

[16] A. Singh, C. Kumar, L. G. Kannan, K. S. Rao, and R. Ayothiraman, "Estimation of creep parameters of rock salt from uniaxial compression tests," *International Journal of Rock Mechanics and Mining Sciences*, vol. 107, pp. 243–248, 2018.

[17] D. Wang, J. Liu, G. Yin, and X. Wei, "Test study of creep properties of gas-bearing coal specimens under triaxial compression," *Chinese Journal of Rock Mechanics and Engineering*, vol. 29, no. 2, pp. 349–357, 2010.

[18] J. Zhang, D. Jiang, Y. Zhao, J. Chen, and L. Li, "Analysis of the mechanical characteristics and energy evolution of tectonic coal during the process of step unloading," *Journal of China Coal Society*, vol. 40, no. 12, pp. 2820–2828, 2015.

[19] Y. Zhao, Y. Wang, W. Wang, W. Wan, and J. Tang, "Modeling of non-linear rheological behavior of hard rock using triaxial rheological experiment," *International Journal of Rock Mechanics and Mining Sciences*, vol. 93, pp. 66–75, 2017.

[20] Y. Zhao, L. Zhang, W. Wang, W. Wan, and W. Ma, "Separation of elastoviscoplastic strains of rock and a nonlinear creep model," *International Journal of Geomechanics*, vol. 18, no. 1, article 04017129, 2018.